JGR Oceans

RESEARCH ARTICLE
10.1029/2020JC016708

Special Section:
Midlatitude Marine Heatwaves: Forcing and Impacts

A Global, Multiproduct Analysis of Coastal Marine Heatwaves: Distribution, Characteristics, and Long-Term Trends

Maxime Marin[1,2,3], **Ming Feng**[3,4], **Helen E. Phillips**[1,2,5], **and Nathaniel L. Bindoff**[1,2,5,6]

[1]Institute for Marine and Antarctic Studies, University of Tasmania, Hobart, TAS, Australia, [2]ARC Centre of Excellence for Climate Extremes, Hobart, TAS, Australia, [3]CSIRO Oceans and Atmosphere, Indian Ocean Marine Research Centre, Crawley, WA, Australia, [4]Centre for Southern Hemisphere Oceans Research, Hobart, TAS, Australia, [5]Australian Antarctic Program Partnership, Hobart, TAS, Australia, [6]CSIRO Oceans and Atmosphere, Hobart, TAS, Australia

Abstract Major marine heatwave (MHW) events have caused catastrophic impacts on coastal marine ecosystems. However, to date there has not been a global assessment of MHWs in coastal areas where rich marine ecosystems are at risk. Here, we combine four satellite Sea Surface Temperature (SST) products to quantify the distribution, characteristics, and decadal trend of coastal MHWs, using an ensemble approach. Hotspots of MHW stress, defined as yearly cumulative intensity, were found to be concentrated in mid latitude coasts like the Mediterranean Sea, Japan Sea, and Tasman Sea, as well as the north-eastern coast of the United States. We found a global increase in coastal MHW frequency and duration during the past 25 years by 1–2 events per decade and 5–10 days per decade, respectively, with regional distribution closely related to decadal climate variability. Increases in frequency and duration of MHWs has led to large increases of cumulative intensity and yearly cumulative intensity, particularly in mid-latitudes and hotspot regions. Long-term changes in mean SST were the main driver of the observed trends of coastal MHWs, while internal variability was important for explaining local decreases in MHW metrics such as along the south-eastern Pacific coast. MHW average metrics and trends were consistent across all four products used in this analysis, giving high confidence in the results. However, important differences between products were observed for MHW mean intensity, which was well correlated to SST variability, suggesting sensitivity of this metric to the specific SST data set and demonstrating a need for an ensemble approach to MHW analysis.

Plain Language Summary Despite marine ecosystems having recently been severely impacted by marine heatwave (MHW) events, there is still a lack of MHW studies in coastal areas. Here, we use a combination of four Sea Surface Temperature (SST) global products derived from satellite measurements, to provide the best estimation of MHW characteristics and long-term changes during the last 25 years. We found that hotspots were concentrated along the Mediterranean Sea, Japan Sea, south-eastern Australia and the north-eastern coast of the United States. We also found that the frequency of MHW events and their duration globally increased by 1–2 events and 5–20 days per decade, respectively. Most of the MHW hotspots identified were associated with high trends. The main driver of long-term MHW increase was long-term changes in SST which, in the context of climate change, has been steadily increasing. In some regions like the south-eastern Pacific coast, long-term changes of MHWs were driven by the local variability of the climate system. All SST products used in this analysis agreed well, except for MHW mean intensity, which was found to be well correlated to short-term SST variations, reminding us of the specificities of SST products and the importance of combining them to reduce uncertainty.

Key Points:

- Global assessment of coastal MHWs using an ensemble of four daily Sea Surface Temperature (SST) products
- Coastal MHW hotspots in terms of simple and cumulative metrics were concentrated in the mid-latitudes
- Along most coastlines, increasing MHW exposure during the last 25 years is driven by long-term warming of SST

Supporting Information:

- Supporting Information S1

Correspondence to:
M. Marin,
Maxime.Marin@csiro.au

Citation:
Marin, M., Feng, M., Phillips, H. E., & Bindoff, N. L. (2021). A global, multiproduct analysis of coastal marine heatwaves: Distribution, characteristics and long-term trends. *Journal of Geophysical Research: Oceans*, *126*, e2020JC016708. https://doi.org/10.1029/2020JC016708

Received 11 AUG 2020
Accepted 28 DEC 2020

1. Introduction

In the context of global warming, extreme events in the ocean have recently received much attention among the scientific community. In the oceans, marine heatwaves (MHWs) have recently gained notoriety among the scientific community primarily due to their catastrophic impact on ecological communities (Collins et al., 2019; Garrabou et al., 2009; Wernberg et al., 2012) and fisheries productivity (Pearce et al., 2011) around the globe. MHWs are discrete events characterized by strong positive temperature anomalies driven by atmospheric and/or oceanic processes.

The majority of MHW studies have focused on unique events that had considerable impacts on marine communities. In summer 2003, a MHW in the Mediterranean resulted in mass mortality of benthic invertebrates (Garrabou et al., 2009) and seagrass (Sparnocchia et al., 2006). During austral summer 2011, a strong *La Nina* event forced an unprecedented warming of the Leeuwin Current (Feng et al., 2013) causing widespread coral bleaching (Gilmour et al., 2013), increased mortality rates of cooler water benthic species (Smale & Wernberg, 2013; Wernberg et al., 2012), and extreme disruption to the fishery industry (Caputi et al., 2019). Another major MHW event in the northeast Pacific known as "the Blob," during boreal winter of 2013–2014, was strong enough to impact marine mammals and sea birds (Cavole et al., 2016) and disrupt weather patterns on the west coast of the United States (Bond et al., 2015). Globally, many of the documented MHW occurrences have been attributed, to some degree, to the main climate modes of variability (Holbrook et al., 2019).

Although the characteristics, physical drivers and ecological impacts of those events are now better understood, MHWs are still largely understudied compared to their atmospheric counterparts. In particular, the focus of the MHW research mentioned above can be interpreted as a focus on MHW "hotspots" (Holbrook et al., 2019), when in fact MHWs are likely to develop in every part of the world. Global MHW assessments are needed to compare the relative impact and strength of MHWs across basins and identify where their associated stress on marine communities and change are the largest.

A study by Oliver et al. (2018) began to address the lack of global assessment by comparing the relative MHW exposure (e.g. frequency and duration) and the average MHW intensity in the global ocean using a satellite Sea Surface Temperature (SST) and a historical SST data set. They found that although MHW frequency was homogenous, MHW intensity (associated temperature anomaly) peaked in high SST variability regions and MHW duration was longer in the eastern Pacific, largely due to the main influence of El Nino/Southern Oscillation (ENSO) on SST variability. The authors also highlighted that MHW frequency and duration had been significantly increasing globally during the last century by 34% and 17%, respectively, leading to an increase in MHW days of 54%. These increases in MHW exposure were mainly attributed to the rising SST trend due to anthropogenic forcing using observations (Oliver, 2019) and future climate projections (Oliver et al., 2019).

Despite the significance of these recent results, further work is needed to capture a complete assessment of MHW characteristics and their impact on marine ecosystems. First, MHW exposure and intensity have only been investigated separately. A more robust representation of MHW potential impact on marine communities can be obtained by combining both exposure and intensity of MHWs. Some marine species might be sensitive to high exposure of small intensity MHWs, while others to a low exposure of high intensity MHWs. Second, coastal ecosystems, with a typical depth of less than 100 m, are the richest and most complex ecosystems in the ocean (Costello & Chaudhary, 2017). Global ocean analyses tend to overlook coastal zones as coastal features are very small relative to the large-scale temperature anomaly patterns. Finally, the majority of MHW studies, including these recent global assessments, only used the National Oceanic and Atmospheric Administration (NOAA) Optimum Interpolation SST (OISST) product. Several other long-term daily SST reanalysis products exist, and, despite the use of similar observations, there are well known differences between them. Among the large variety of SST products, the OISST product often differs the most with in-situ observations such as Argo (Fiedler et al., 2019), undermining its use in MHW analyses.

In light of the recent MHW work, this study examines MHW distribution and impact in coastal environments, investigating their representation across four satellite daily SST reanalyses. In addition, changes in the relative stress to coastal ecosystems of MHWs during the last 25 years are investigated. Lastly, we aim to quantify the relative contributions of both anthropogenic long-term change in mean SST and internal variability to the observed MHW changes.

2. Methods

2.1. Satellite Temperature Datasets

We performed a global MHW coastline analysis using four daily global L4 (gap-free, gridded) SST analysis products covering at least 25 years. The products included: NOAA Advanced very High Resolution Radiometer (AVHRR) Optimum Interpolation (OI) ¼ degree daily SST v2.0 Analysis data (Reynolds et al., 2007);

Table 1
List of Daily Satellite Temperature Datasets Used in the Study

Product	Time coverage & resolution	Spatial resolution (°)	Depth
OISST Reynolds et al. (2007)	01/09/1981–present daily	0.25 × 0.25	0.1 m
MGD Sakurai et al. (2005)	01/01/1982–present daily	0.25 × 0.25	foundation
CMC Brasnett (2008)	01/09/1991–17/03/2017 daily	0.2 × 0.2	foundation
CCI Merchant et al. (2019)	01/09/1981–31/12/2016 daily	0.05 × 0.05	0.2 m

CCI, Climate Change Initiative; CMC, Canadian Meteorological Center; MGD, Merged satellite and in-situ data Global Daily; OISST, Optimum Interpolation SST; SST, Sea Surface Temperature.

Japan Meteorological Agency (JMA) Merged satellite and in-situ data Global Daily SST (referred to as MGDSST; Sakurai et al., 2005); Canadian Meteorological Center (CMC) 0.2 degree analysis v2.0 (referred to as CMC; Brasnett, 2008); European Space Agency (ESA) SST Climate Change Initiative (CCI) Analysis Climate Data Record v2.1 (referred to as CCI; Merchant et al., 2019). All products are remote sensing based including adjustments to satellite bias with respect to a variety of in situ data from ship, drifting buoys, and/or moorings.

A summary of information for each data set is provided in Table 1. CMC had the shortest time coverage, starting in 1991 and ending in 2016. For the purpose of comparison between products, data used in our analysis were restricted to 01/01/1992–31/12/2016. Coastline pixels from each data set were derived as the closest pixel to a coastal node that was not contaminated by land in the intermediate-resolution GSHHS (Global Self consistent, Hierarchical, High-Resolution Shoreline) database (Wessel & Smith, 1996). Multi-product means were computed by averaging OISST and MGD coastal pixels (identical grid) with the respective closest coastal pixels from CMC and CCI. De-seasoned time series were retrieved by subtracting daily climatologies, calculated over the 25 years period for all products, from the raw time series.

2.2. MHW Analysis

The MHW analysis was conducted using the MATLAB "m_mhw" toolbox (Zhao & Marin, 2019), available (https://github.com/ZijieZhaoMMHW/m_mhw1.0), which follows the MHW definition specified in Hobday et al. (2016). The authors defined a MHW relative to a local baseline climatology, using an 11-day moving window centered on the specific time of the year. This allows for the existence of MHWs not only during hot summer months and takes into consideration the local variability of temperature. The baseline climatology should span a minimum period of 30 years so as to incorporate low frequency climate modes of variability which can prove determinant in the genesis and development of MHWs. Such climate modes include ENSO (Feng et al., 2015; Scannell et al., 2016; Zhang et al., 2017) and the Atlantic Multi-Decadal Oscillation (AMO; Scannell et al., 2016). From the climatology, threshold temperature values for each location are calculated using the 90th percentile rather than an absolute value, further taking into consideration the difference in temperature variability between regions. In our research, the baseline climatology was defined as the 1992–2016 (25 years) time series at each location. Although Hobday et al. (2016) recommend that the baseline climatology span a minimum period of 30 years, the shorter time coverage of CMC limited our period to 25 years.

Unlike most past MHW studies, long-term SST trends were removed from the time series prior to the calculation of the climatology, which removes the contribution from the SST trend to its variance and effectively reduces the SST variability range. This allows for a better representation of the climatological state at the beginning of the study period (1992) and of the impact of long-term change on MHWs during the last 25 years. For clarity, we define this climatology as "Climatology_1992." Note that the original SST time series were still used in the MHW calculation. Figure 1 shows an example of the effect of this methodology at three typical locations. In the Black Sea, using Climatology_1992 to calculate MHW thresholds resulted in a sharp increase in both the average and trend of MHW yearly cumulative intensity, as compared with the normal climatology (Figure 1a). However, there were no significant differences in trend and average of MHW yearly cumulative intensity at the tropical east Pacific location (Figure 1b), which are dominated by

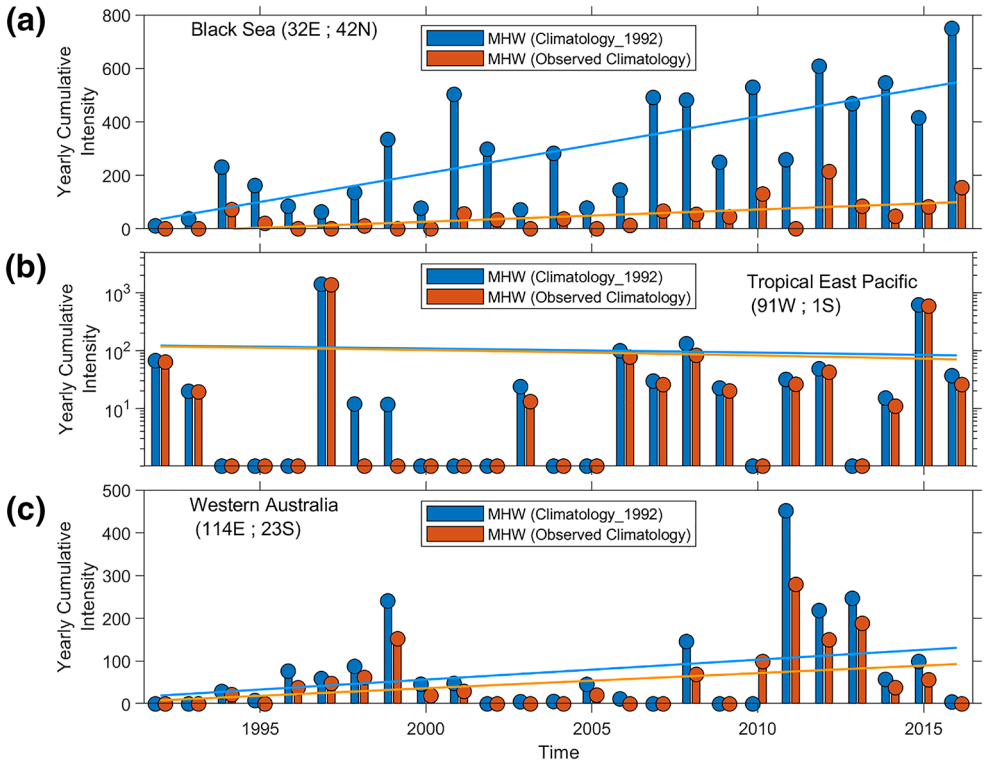

Figure 1. MHW yearly cumulative intensity (°C days year^{-1}) time series at (a) 32°E, 42°N, (b) 91°W, 1°S, and (c) 114°E, 23°S. MHW yearly cumulative intensities were derived from the NOAA OISST v.2 product data from 1992 to 2016, using the Hobday et al. (2016) MHW definition (red). Climatologies calculated from detrended SST time series were used to derive a second MHW yearly cumulative intensity time series (blue). Removing linear trends from SST time series allows MHW threshold calculations relative to the start of the study period (e.g. 1992). Linear regressions of MHW yearly cumulative intensity time series were overlayed. Linear regression coefficients a such as $y = ax + b$ were (a) ~21.32 and ~4.6, (b) −1.62 and −1.98, and (c) 4.65 and 3.53°C days year^{-1} per year for the detrended and observed time series, respectively. MHW, marine heatwave; NOAA, National Oceanic and Atmospheric Administration; OISST, Optimum Interpolation SST; SST, Sea Surface Temperature.

the two strong El Nino events. Those contrasting results were explained by the difference in SST trends at the two locations, as the Black Sea was associated with a strong positive long-term trend during the last 25 years while SST trend in the tropical east Pacific was weak (Figure 1b). In the case of a moderate positive SST trend like in western Australia, the difference in MHW trend and average was smaller than in the Black Sea, but still noticeable (Figure 1c).

Finally, we adopt the following additional constraints on the analysis: (1) locations with SST lower than −1°C were removed from the analysis due to possible contamination from sea-ice; (2) a MHW event can be no shorter than five consecutive days, following Hobday et al. (2016) to achieve uniform MHW counts globally under current climatic conditions; and (3) two MHW events are considered as a single event if the gap between them is less than 2 days.

The MHW analysis returns specific sets of metrics, including duration, mean intensity, maximum intensity, cumulative intensity (measured in degree days), and the date at the start, peak, and end of each event (Hobday et al., 2016). As mean and maximum intensity were highly correlated (not shown), only mean intensity was used in the study. Annual MHW days were calculated to measure ecosystem exposure to MHWs. Cumulative intensities were summed to derive yearly cumulative intensities. The potential impact of individual events on marine ecosystems is best represented by their cumulative intensity, combining the effect of duration and average intensity. However, yearly cumulative intensities measure the long-term stress induced by MHWs on the environment and therefore including the effects of frequency of events. Note that dates used throughout the study only refer to the peak date of events. Trends in characteristics of MHWs were

derived from linear regressions. Trends of yearly frequency were derived using a generalized linear model to account for the Poisson distribution characteristic for count data, using the log link function. The use of linear models may present unusual biases due to the specificities of MHW data metrics being bounded to lower values like duration (5 days minimum) or intensity (equal to threshold at minimum). Long-term changes can be estimated using the difference between the mean of two time periods, but it would not capture the full extent of MHW data. Regardless, we tested both approaches and found similar temporal trends and spatial patterns (not shown).

2.3. Evaluation of SST Long-Term Trend Impact

Total variability can be decomposed into a decadal trend and interannual variability. While long-term trends are most likely dominated by external forcing, internal variability can play an important role in regulating the climate on shorter timescales. SST Internal variability was isolated by removing the linear trend from the time series at each individual pixel. The "observed" SST can be reconstructed by adding back the linear trend to the detrended SST time series. The MHW algorithm with the same base climatology (Climatology_1992) was then run on the two datasets, the observed SST time series with both long-term trends and internal variability, and the detrended time series (Figure A.1, supporting information). The latter contained information on MHWs that would have happened relative to the 1992 state of the oceans, without any long-term SST trend (i.e. solely due to internal variability). Running the MHW algorithm using detrended climatologies on detrended time series (red line-Figure A.1, supporting information) and observed climatologies on observed time series (red line-Figure 1) yielded similar, yet different, results. In both cases, the long-term trend signal in annual MHW metrics was minimized in different ways. To isolate the influence of the long-term trends of SST on any MHW metric, the internal variability component was subtracted from the observed metric:

$$X_{\Delta SST} = X_{ob} - X_{IV}$$

where X_{ob} and X_{IV} are MHW metrics calculated from the observed SST time series and the detrended SST time series, respectively.

Assessing the influence of climate change on MHW trends relies on separating the trend components from the decadal trend and internal variability. An attributional ratio was derived to measure the relative influence of both at every location:

$$\text{Trend attributional ratio} = \frac{\left|T_{\Delta\text{SST}}\right| - \left|T_{IV}\right|}{\max\left(\left|T_{\Delta\text{SST}}\right|, \left|T_{IV}\right|\right)}$$

Here, |...| is the absolute value operator, and $T_{\Delta\text{SST}}$ and T_{IV} are MHW trends induced from the change in mean SST and from internal variability, respectively. Positive values indicate a stronger influence of a change in mean SST on the observed trends while negative values indicate a stronger influence of internal variability (Figure A.1, supporting information). The ratio was scaled to the highest trend component so that values are bounded between −1 and 1 to indicate the relative contribution of each forcing. A trend attributional ratio value of 0 indicates that changes in mean SST and internal variability were equally driving observed trends in MHW characteristics, while a value of 1 (−1) indicates that the change in mean SST (internal variability) was the only driver of the observed trend.

2.4. SST Product Comparison

The differences of MHW representation within different SST products have not been previously investigated. All SST products are unique in multiple ways and have biases that very likely transfer into MHW calculations. In this study, for each coastal pixel and MHW metric, individual product values were compared with the multiproduct mean to assess whether a product should be considered an outlier as defined in the following paragraph. If one or more products was identified as an outlier, the location was flagged as one with a significant difference between products.

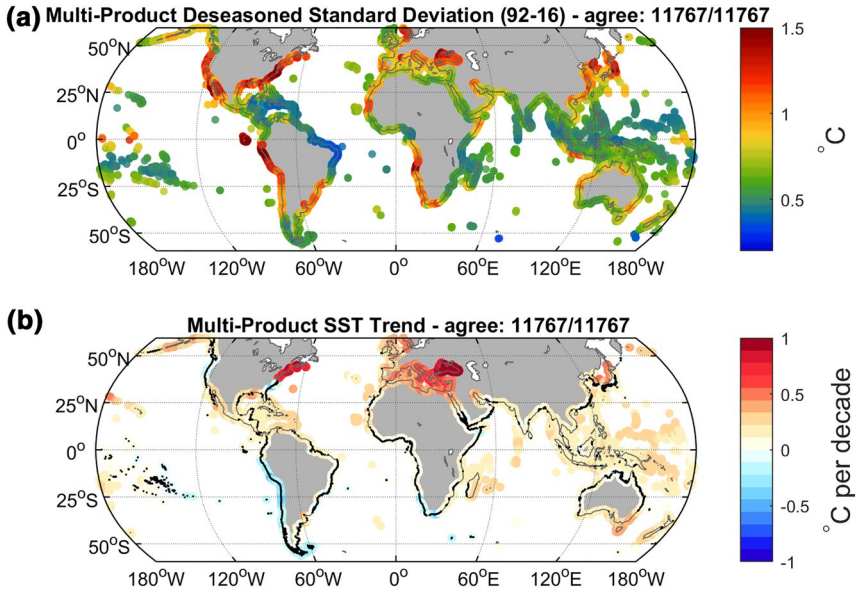

Figure 2. Multiproduct average of (a) de-seasoned standard deviation of SST and (b) linear SST trend over 1992–2016. Black dots denote the locations where trend estimates were not significantly different from zero ($p > 0.05$). The total count of locations where all individual product averages were similar to the estimate of the multiproduct mean (at the 90% confidence level) is indicated. SST, Sea Surface Temperature.

For MHW average metrics, the product associated error was defined as:

$$\varepsilon_i = 1.96 \times \left(\frac{\mathrm{std}(X)}{\sqrt{n}} + \frac{\mathrm{std}(X_i)}{\sqrt{n_i}} \right)$$

where X is the multiproduct data containing yearly averages of MHW metrics for all four products (i.e. 4×25 years), X_i is data from yearly averages of an individual product (i.e. 25 samples) and n is the sample size. Note that the error includes the error associated with the multiproduct mean as well as the error associated with the individual product mean. The individual product was flagged as significantly different than the multiproduct mean, termed an outlier, if the following condition was met:

$$\left| \overline{X} - \overline{X_i} \right| > \varepsilon_i$$

For metrics where yearly averages were not applicable, resulting in four individual values from each product (i.e. trends), the error was defined as 3.5 standard deviations of the four individual product trend values. The value of 3.5 is roughly equivalent to the 95% level of significance for a two-tailed t-distribution with 3° of freedom. Note that the aim of the study is not to give a precise quantitative assessment of the multiproduct error but to show where the four products are unanimous and where there is a deviation from the multiproduct mean.

3. Results

3.1. SST Overview

Multiproduct averages of de-seasoned SST variability and linear SST trends are shown in Figure 2. De-seasoned SST variability was globally weaker in the tropics (~0.5°C), reaching a minimum along the western tropical Atlantic coast (Figure 2a). Variability increased in mid to high latitudes, especially along the western and eastern boundary currents reaching 1–1.5°C. Maximum values of de-seasoned SST variability were observed in the equatorial eastern and south-eastern tropical Pacific (>1.5°C), due to ENSO variability.

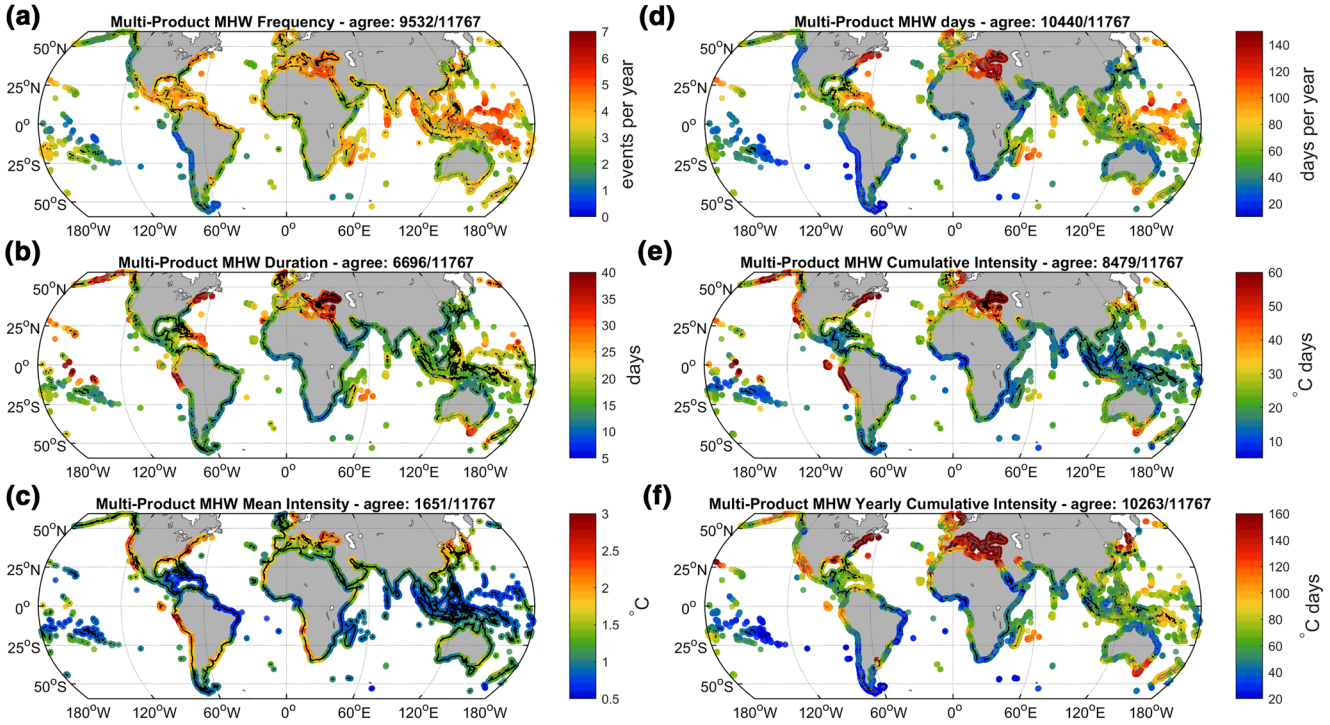

Figure 3. Multiproduct average of (a) MHW frequency, (b) MHW duration, (c) MHW mean intensity, (d) MHW days, (e) MHW cumulative intensity, and (f) MHW yearly cumulative intensity over 1992–2016. Locations where the average of at least one product was flagged as different are marked by the black dots. The total count of locations where all individual product averages were similar to the estimate of the multiproduct mean (at the 90% confidence level) is indicated. MHW, marine heatwave.

Other regions of high de-seasoned SST variability include mid-latitudinal semi-enclosed seas such as the East China Sea, Japan Sea or the Black Sea (Figure 2a).

Multiproduct linear trends of SST were mostly positive along the coastlines, on the order of a few tens of degrees per decade (Figure 2b). The highest increase in SST was observed in the Black Sea where SST warmed by more than a degree per decade over the 1992–2016 period. Strong positive trends of ~0.75 degree per decade were also observed along the north-eastern coast of the United-States (hereafter denoted NE-US). Weaker positive SST trends were observed in some tropical areas like northern Australia, north-eastern Indian Ocean and the eastern tropical Atlantic Ocean. Some coastal regions were characterized by a cooling of SSTs. Indeed, the south-eastern Pacific showed the strongest decrease of up to 0.3 degree per decade, which might be associated with the global warming hiatus during 1998–2014 as the Pacific climate shifted to a more-La Nina like condition (Kosaka & Xie, 2013). Some parts of the north-eastern Pacific coast (40°N–50°N), north-western (30°N–35°N) Atlantic coast and in the southern Atlantic were also characterized by a long-term decrease in SST.

3.2. MHW Average Properties

Average characteristics of MHWs during the last 25 years are shown in Figure 3 and discussed individually below. Although events happen everywhere, by definition, some coastal regions are more vulnerable to MHWs than others. Note that similarities between products for all MHW metrics and trends will be discussed in Section 3.5.

3.2.1. Frequency

MHWs were more frequently observed along tropical coastlines (Figure 3a). On average, 5–6 events per year have occurred in the western tropical Pacific during the last 25 years. A high number of events were also observed in the Mediterranean Sea (5 events per year). In contrast, eastern boundary regions had many fewer events, especially on the eastern Pacific coast and extending to the central Pacific, where less than 2

events per year were observed on average. This distribution can be, to some extent, explained by SST variance as the low-frequency variability of ENSO can be associated with a low frequency of MHW events in the eastern Pacific, while higher frequency noise will also likely influence SST variability in the tropics and enclosed seas.

3.2.2. Duration

The analysis of MHW average duration highlighted clear hotspots of long-lasting MHWs. The longest average MHW events occurred in the eastern Mediterranean Sea, the Black Sea and along the NE-US. The average duration of events in those two regions was up to 40 days (Figure 3b). Other regions such as the North Sea, the Tasman Sea, the Lesser Antilles, the southwest Indian Ocean and parts of the north-east Pacific are characterized by long duration MHWs of 25–30 days on average. Elsewhere, duration ranged from 10 to 15 days. While analogously to frequency, the main modes of variability can potentially explain average MHW duration values in some locations like the central-north-eastern Pacific, we note that the correlation between both MHW frequency and duration with de-seasoned SST variability was extremely weak (Figure A.2, supporting information).

3.2.3. Mean Intensity

There was a distinct difference in multiproduct MHW mean intensity between the tropics and mid-latitudes (Figure 3c). MHW mean intensity was low in the tropics, typically less than 1°, and maximum in mid-latitudes, reaching 2.5° along mid-latitude marginal seas and active boundaries of the Atlantic and eastern Pacific oceans (Figure 3c), and lower again at high latitudes (>45°). Mean intensity was highly correlated with de-seasoned SST standard deviation across all four products ($R^2 = 0.94$; Figure A.2c, supporting information), suggesting that average MHW intensities are closely related to temperature variability. Indeed, unlike MHW threshold calculations, MHW intensity measures are not scaled relative to local temperature variability (Hobday et al., 2016) but are simply the difference between the observed temperature and the climatology. Therefore, coastlines with strong intraannual variability such as western boundary currents and enclosed seas and/or strong interannual variability, such as the south-eastern Pacific, are more likely to experience MHWs with high intensities. This result is also consistent with the time of emergence of climate change in the oceans. That literature shows that regions where the time of emergence is earlier is also where the internal variability tends to be smaller (Bindoff et al, 2014), analogous to the lower intensity shown here (approximately equivalent to internal variability in time of emergence calculations).

3.2.4. MHW Days

The number of MHW days per year displayed in Figure 3d showed that the highest yearly average was observed in the eastern Mediterranean Sea, including the Black Sea, and the NE-US. During the last 25 years, MHWs occurred, on average, more than 150 days per year in those regions (Figure 3d). Other MHW days hotspots included the western tropical Pacific, the Tasman Sea, the southwest Indian Ocean and the Lesser Antilles, averaging between 100 and 120 MHW days per year. These values are significantly higher than the theoretical maximum number of MHW days per year of ∼36 days that a 90th percentile threshold preconditions. This is explained by our choice of setting the MHW threshold based on detrended climatologies (Figure 1) allowing for a much higher number of MHW days per year when there is an underlining warming trend. MHW days hotspots were usually associated with MHW duration hotspots (Figure 3b) whereas the relationship with MHW frequency (Figure 3a) was not so apparent. However, linear regression of MHW days with event frequency and MHW duration gave R^2 coefficients of ∼0.73 and ∼0.52, respectively (Figure A.3, supporting information), indicating that MHW days were better correlated with event frequency than MHW duration. The importance of MHW frequency was particularly evident in the western tropical Pacific, where MHW duration (Figure 3b) was moderate but MHW frequency was the highest of any region (Figure 3a), resulting in high values of MHW days. A contrasting example was the south-eastern tropical Pacific, where MHW duration was high but MHW frequency was the lowest on average, resulting in low values of MHW days.

3.2.5. Cumulative Intensity

Individual event strength is potentially better represented by the cumulative intensity metric combining both its duration and intensity. The multiproduct average of mean MHW cumulative intensity showed that

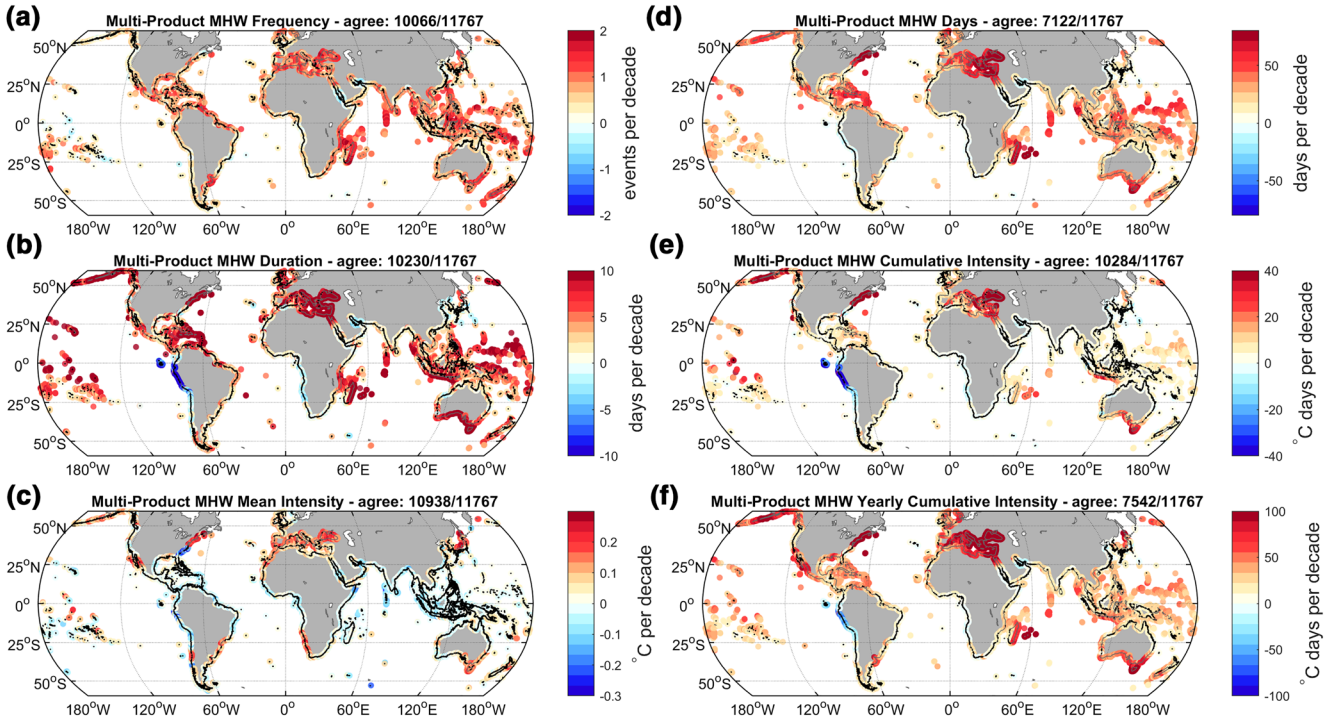

Figure 4. Multiproduct average trends over 1992–2016 of (a) MHW frequency, (b) MHW duration, (c) MHW mean intensity, (d) MHW days, (e) MHW cumulative intensity, and (f) MHW yearly cumulative intensity. Black dots denote the locations where trend estimates were not significantly different from zero ($p > 0.05$). The total count of locations where all individual product averages were similar to the estimate of the multiproduct mean (at the 90% confidence level) is indicated. MHW, marine heatwave.

the strongest MHW events were located in the eastern Mediterranean Sea, the Black Sea, the NE-US and along the south-eastern tropical Pacific coast. Values of cumulative intensity of events reached on average more than 60 degrees days (Figure 3e). MHW cumulative intensity was lowest in the tropics (10 degrees days) but increased in mid latitudes. The north-eastern Pacific coast had remarkably strong events, ranging from 35 to 50 degrees days (Figure 3e). MHW cumulative intensity values were positively correlated with duration and mean intensity (R^2 of ~0.55 and ~0.54, respectively; Figure A.3, supporting information) and we note that they are both essential for explaining the distribution of cumulative intensity.

3.2.6. Yearly Cumulative Intensity

Perhaps the most important MHW metric in assessing MHW associated risks on the environment is yearly cumulative intensity. The highest values of yearly cumulative intensity are observed in European Seas and the NE-US, where the annual stress reached on average more than 160 degrees days per year (Figure 3f). Secondary hotspots with values ranging from 120 to 140 degrees days per year included the Tasman Sea, the Japan Sea and the northern Caribbean Sea. High values of yearly cumulative intensity were associated with strong individual events (Figure 2e). The better predictor of yearly cumulative intensity was MHW duration ($R^2 \sim 0.6$) as frequency and mean intensity did not correlate well (Figure A.3, supporting information). However, frequency might be important in some regions like the western tropical Pacific, which were characterized by weak individual events (10 degrees days; Figure 3e) but moderate cumulative stress (up to 100 degrees days per year; Figure 2f), due to a very high frequency of events (6 events per year; Figure 3a). In contrast, low yearly cumulative intensity values in the south-eastern tropical Pacific were likely related to the low frequency of events observed (less than 1 event per year; Figure 3a).

3.3. MHW Trends

Here we examine the long-term trends changes in the observed records and their impacts on the metric of MHW. Long-term changes in MHW metrics during the last 25 years are shown in Figure 4. Results revealed

a global increase in both frequency of MHWs (Figure 3a) and in duration (Figure 4b) with the notable exception of the tropical eastern Pacific. Frequency of MHW occurrence increased relatively homogenously around the globe by 1–2 events per year per decade. Trends in MHW duration were less homogeneous, with more pronounced increases along the southern Australian coastline, the central and western Pacific, along the northern Pacific coastline, in the tropical Indian Ocean, the Mediterranean and Black Seas, the Lesser Antilles and along the NE-US, typically gaining 10 days per decade over the last 25 years. Despite overall positive trends in most regions, small isolated decreases in frequency and duration were observed, especially along the south-eastern tropical Pacific coastline, where the average duration of events decreased by more than 10 days per decade (Figure 4b). Global increases in MHW exposure induced an increase in MHW days (Figure 4d). The highest increase corresponded with the highest increase in duration as changes in frequency were more homogenous. In these regions, MHW days increased by more than 50 days per decade, which, assuming a constant increase and initial values of 60–100 MHW days on average (Figure 3d), would force SST into a permanent MHW state in roughly 50 years (e.g. by approximately 2055 if relative to the middle of 1992–2016).

MHW mean intensity trends are globally weak and, unlike MHW frequency and duration, have not been increasing globally (Figure 4c). Significant increases were observed in mid-high latitudes. In the northern hemisphere, increases were concentrated along the shores of enclosed seas such as the Mediterranean Sea, the Japan Sea, and Baja Sea, and in the NE-US. MHW mean intensity has also increased in some parts of the southern hemisphere coastlines, including the south Atlantic and south-eastern Australian coastlines. In those places, the MHW mean intensity increase ranged from 0.1 to 0.25 degrees per decade, which is small compared to average mean intensity values which are up to 10 times higher in amplitude (Figure 3c). In the tropics, MHW mean intensity has been slightly decreasing by 0.05–0.1 degree per decade.

Changes in MHW cumulative intensity were globally positive (Figure 4e). Regions with very high trends had the highest change in cumulative intensity, including the south-eastern Australian coastline, the eastern Mediterranean Sea, the Black Sea, the NE-US coast, the central and northern Pacific (Figure 3e). MHW cumulative intensity in those regions increased by more than 40 degrees days per decade during the last 25 years. Note that these cumulative intensity trend hotspots were also hotspots for average cumulative intensity. In contrast, most other parts of the world, including the tropics, have seen smaller cumulative intensity increases ranging from 0 to 15 degree days. The slight trend in decreased MHW mean intensity (Figure 4c) might explain the dampened cumulative intensity trend in the tropics. The strongest decrease in MHW cumulative intensity (Figure 4e) along the south-eastern tropical Pacific of more than 40 degrees days per decade results from the shortened duration of MHWs in that region (Figure 4b).

MHW yearly cumulative intensity increased along most coastlines (Figure 4f). Regions with high positive trends in MHW cumulative intensity (Figure 4e) were associated with strong increases in MHW yearly cumulative intensity of more than 100 degrees days per decade. In the Tropics, the increase of MHW frequency increased yearly cumulative intensity by around 25–50 degrees days per decade. The only decrease of MHW yearly cumulative intensity was observed along the south-eastern tropical Pacific coastline, consistent with a decrease of cumulative intensity (Figure 3e). Although MHW metric trends were consistently negative in this region, they were not significant. A strong MHW event towards the beginning of the 1992–2016 time period (1998; Figure 1b), most likely caused by the extremely strong 97–98 El-Nino event (Vecchi & Harrison, 2006), created a huge bias in the linear trend of south-eastern Pacific cells, where low-frequency SST variability and a small number of events made MHW trends highly sensitive to outliers. We note that other strong El-Nino's, like the 2015–2016 event, might have highly influenced MHW trends in more central Pacific cells, as its warming signature was centered more towards central Pacific (Santoso et al., 2017).

3.4. Drivers of MHW Trends

Figure 5 shows the MHW TAR. This metric attributes the proportion of MHW evolution over the last 25 years that is due to long-term changes in mean SST and due to the remaining internal variability. Positive values indicate that change in mean SST is the dominant driver of the trend; negative means that internal variability is the dominant driver. Frequency and duration trends were mostly explained by the long-term changes in SST (Figures 4a and 4b). A dominance of internal variability was observed along coastlines where MHW frequency and duration decreased or remained the same (Figures 4a and 4b) such as most of the central and

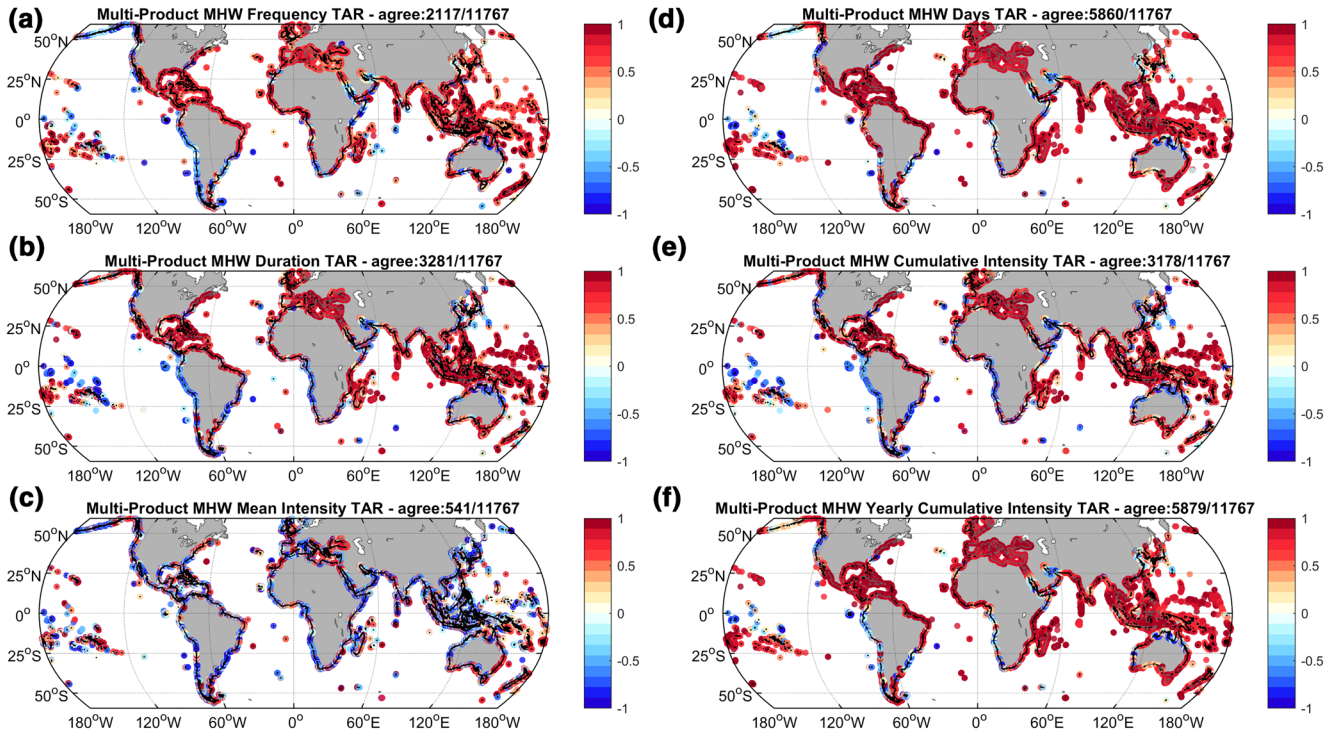

Figure 5. Trend Attributional Ratio (TAR) of the multiproduct trends of (a) MHW frequency, (b) MHW duration, (c) MHW mean intensity, (d) MHW days, (e) MHW cumulative intensity, and (f) MHW yearly cumulative intensity. Positive values indicate a stronger influence of mean SST change on the observed trends while negative values indicate a stronger influence of internal variability. Black dots denote the locations where the TAR sign of at least one SST product was different than the others. The total count of locations where all products have the same TAR sign is indicated. MHW, marine heatwave.

eastern Pacific, the southern Atlantic, the northern Australian coast and parts of the north-western Indian Ocean. While some of those regions are associated with weak SST trends, explaining the small impact of long-term changes in the mean, there was a significant decrease of SST along the south-eastern Pacific coast (Figure 2b). Results suggest that decreases in SST along the south-eastern Pacific were not the main driver of the decrease in MHW frequency and duration, but that rather, internal variability processes have favored shorter and less frequent events in recent years.

The MHW Days trend in most locations was primarily driven by long-term changes in SST (Figure 5d). Internal variability remained the major contributor to the trend in MHW Days in regions where it explained the frequency and duration trends (Figures 5a and 5b). However, there was an exception along the southeast Pacific coast where trends in MHW exposure were mostly driven by long-term changes in SST (Figure 5d), while both frequency and duration trends were mostly explained by internal variability processes (Figures 5a and 5b). A possible explanation is that changes linked to internal variability induce an absence of significant change in MHW exposure. Indeed, the south-east Pacific coast is characterized by a small increase in MHW frequency (Figure 4a) but a large decrease in duration (Figure 4b). Since an event's duration is on average very long here (Figure 3b), a small increase in frequency can lead to a large increase in MHW exposure overwhelming the effect of the decrease in event duration. Therefore, the MHW exposure trend in the southeast Pacific is less affected by internal variability processes and is dominated by long-term SST cooling (Figure 5d).

Trends in MHW mean intensity were largely explained by internal variability, as attributional index values were globally negative (Figures 4c and 4d). This confirms that MHW mean intensity is closely related to local processes that affect SST. Positive index values were however found in the eastern Mediterranean Sea, the Black Sea and the NE-US, where the highest increases in mean SST were observed (~1 degree per decade, Figure 2b). The warming of SSTs in these regions was likely large enough to force a response in MHW intensity changes.

Both cumulative intensity and yearly cumulative intensity trends were largely explained by long-term trends in SST (Figures 5e and 5f). Nevertheless, internal variability remained important in regions with negative/small observed trends (i.e. most of the central and eastern Pacific, the southern Atlantic, the northern Australian coast and parts of the north-western Indian Ocean). Regions with negative MHW trends were often associated with a decrease in SST (Figure 2b).

3.5. SST Product Differences

The four SST products that we used in this analysis are the result of different algorithms and approaches to the SST data to create a product. By using several available products, we are also able to assess the differences in the products to establish potential biases, differences in smoothing and differences in MHW metrics. Like IPCC, we prefer an ensemble approach to all of the SST products, thus ensuring an objective analysis. It also increases the likelihood that the ensemble mean is more accurate than any single product and implicitly takes into account algorithmic biases in these collections. Average MHW metrics from the four SST products were generally similar, indicating that the average MHW state is consistent across the globe and increasing our confidence in hotspot locations (Figure 3). Only MHW mean intensity showed major differences between products as only ∼15% of locations had no significant differences between individual SST product means and the multiproduct mean (Figure 3c). This suggests that, although de-seasoned SST variance estimations were judged similar among products (Figure 2a), those small variance dissimilarities might have transposed into larger MHW mean intensity differences. Therefore, estimations of MHW mean intensities can differ largely depending on the choice of SST product. Note that MHW duration estimations, although much more similar across SST products (>50% similarity), showed some differences, especially in the western Pacific warm pool, the Caribbean and, importantly, in the north-eastern Mediterranean Sea, including the Black Sea, where the highest values were observed (Figure 3b). These differences in MHW duration led to differences in MHW cumulative intensity estimations (Figure 3e).

All SST products used in this study gave similar estimates of MHW metric trends across most locations (Figure 4), increasing the confidence in the multiproduct trends. On the other hand, the relative impacts of trends in the instrumental record and internal variability, given by the TAR, differed widely among products (Figure 5). Similarities were only observed in the Mediterranean Sea, the NE-US coast and western Pacific. The high similarity of MHW trend estimates by individual products (Figure 4) contrast with the poor similarity of TAR values, suggesting that the internal variability of MHWs is not captured evenly in all products. This is further highlighted by the fact that locations where MHW trends were mostly influenced by internal variability were consistently flagged as locations where the products disagreed on the dominance of long-term or internal variability. In addition, based on its definition, the sign of TAR is more likely to differ among products where the long-term trends are weak, as is the case globally for mean intensity. However, the global pattern of TAR values for all MHW metrics was consistent throughout all four satellite products (not shown), including MHW mean intensity (Figure A.5, supporting information), for which most coastal pixels product-comparison was flagged as different (Figure 5c). In all four products, TAR values were globally negative despite the evidence of spatial noise. When considering a similar TAR sign in at least three products, more than half of the total number of coastal grid points were flagged (Figure A.6, supporting information), showing improved agreement when trying to partially eliminate the noise.

4. Discussion

Our analysis of average MHW characteristics and trends across four different satellite SST products identified the locations of metric-dependant MHW "hotspots" along the world's coastlines. It also revealed that the increasing tendency of MHW individual and prolonged thermal stress on coastal ecosystems, was mostly forced by the long-term changes in SST at these locations.

Our study delivers a more precise analysis of MHW behavior in coastal areas, which are often overlooked in global studies despite their ecological and economic importance. Indeed, it was found in previous studies that coastal SST rates of warming during the last 35 years were more than twice as high as the global ocean warming (Lima & Wethey, 2012), highlighting the greater vulnerability of coastal areas and the need

to investigate them separately from the global ocean. Although coastal pixels are included in past global MHW studies (Holbrook et al., 2019; Oliver, 2019; Oliver et al., 2018), results are focused on a regional to ocean basin scale, which differ from results presented here. For example, those studies identify the Gulf Stream current region as a main hotspot for MHW, but the difference of MHW characteristics between the coastal and open ocean conditions are indistinguishable on global ocean colormaps (Oliver, 2019; Oliver et al., 2018) or regional averages (Holbrook et al., 2019). Here, by focusing on coastal pixels only, we provide an analysis of near-shore MHW conditions and adopt a more refined spatial analysis scale.

In our study, each MHW threshold was calculated based on detrended time series (Climatology_1992), yielding estimates of MHW thresholds at the start of the 25-year period. This differs from the general definition of MHWs described by Hobday et al. (2016), which does not separate the impact of long-term trends from threshold calculations. Our approach allows for a better representation of the relative impact of temperature trends on MHWs and greater insight into the drivers of MHWs. As a result, the Mediterranean Sea and NE-US, where SST trends were among the highest during the last 25 years, were identified as clear hotspots of MHW days and intensity (Figure 3). These locations were not identified as such in previous studies and were rather associated with moderate MHW frequency and duration averages relative to the rest of the world (Holbrook et al., 2019; Oliver et al., 2018), potentially underestimating MHW associated risk on marine ecosystems. The study of long-term trends in MHWs faces some challenges linked to the very definition of a MHW. A shift in the mean SST is followed by a shift of the 90th percentile, increasing/decreasing the threshold value resulting from warming/cooling of SST. In the case of extreme warming, such as in the Mediterranean Sea (Figure 1b), this leads to increases of MHW days of up to 120–140 days per year (Figure 2d) which is not considered as an extreme anymore. However, this shows that what was an extreme event at the start of the studied period (1992), has become normality within 12.5 years, largely due to the intense warming trends. It has been suggested that MHWs be calculated relative to a moving climatology to account for SST trends (Jacox, 2019). In our case, SST time series are too short to allow for moving climatologies in the context of MHWs. Moreover, ecosystem responses to long-term environmental changes are likely highly species dependent. Our aim is not to give an ecological assessment of MHW impacts, but rather to quantify the physical characteristics of MHWs to better assist future ecological studies and management policies.

In addition to providing basic MHW metrics, our results assess MHWs in terms of cumulative intensity. In most cases, cumulative intensity is a more complete measure of heat stress for marine systems and could be better suited for risk assessment studies, as it combines both MHW duration and intensity. Increases of SST above a certain threshold (i.e. high MHW intensity) can alter coral physiological capabilities (Lough et al., 2018) and, if prolonged (i.e. high MHW duration), can break down the symbiotic relationship of corals with their algae, leading to coral bleaching (LaJeunesse et al., 2018). In fact, most studies investigating heat-stress on coral use a cumulative temperature index called the degree heating week index (Liu et al., 2003). One could argue that MHW cumulative intensity can be computed from multiplying duration with mean intensity. However, the linear relationships are not straight-forward (Figure A.3, supporting information) and can change depending on the local SST variability. A measure of cumulative heat-stress integrated through time, like yearly cumulative intensity, allows the addition of impacts related to the repetition of events. Resilience of coral reefs has been found to be profoundly dependent on the repetition of events, where recurrent events halt the coral recovery and can further diminish the recovery rates of species with slow-recovery metabolism (Thomas et al., 2019). The combined influence of frequency, duration, and intensity of MHWs on marine ecosystems highlights the importance of developing and analyzing new MHW metrics, like cumulative and yearly cumulative intensity, separately. The best example of this is along northern Australia, where heat-stress induced by single events (e.g. cumulative intensity) has not increased during the last 25 years (Figure 4e) while yearly stress (e.g. yearly cumulative intensity) has increased (Figure 4f), resulting in increased coral bleaching. This echoes the increased frequency of bleaching events globally (Hughes et al., 2017).

Changes in MHW characteristics during the last 25 years were found to be largely attributed to long-term SST trends as indicated by the TAR values, excluding MHW mean intensity (Figure 5). While not formally tested, there was no clear evidence that the internal variability had changed in amplitude over the 25-year period of the SST data. Our results compared well with a previous study by Oliver et al. (2019) that used a

different attribution methodology. SST time series in that study were simulated using set values of trends and variance retrieved from an autoregressive model of the observations. This theoretical method tends to overlook the nature of internal variability processes by quantifying the total variability over the time period and translating it into white noise. In our study, a more practical approach is chosen, where we separate the linear trend from all other components of SST variability before computing TAR values. Such an approach does not allow us to estimate the influence of a change in variance, as done in Oliver et al. (2019), but rather compares the influence of long-term changes in SST with all other modes of variability attributed to internal processes of the Earth's climate system.

All attribution studies based on observations are limited by the length of the time series. Some low frequency variability might not be fully captured and could lead to bias in long-term trend estimates. Shortening our time series to a common 25-year time period from the 35 years available in most SST products had little impact on the estimation of the trends (not shown). Additional bias can be created in regions where the amplitude of low frequency internal variability is larger than the amplitude of the trend (Lian et al., 2018). The cooling observed in regions of the east Pacific and south Atlantic from the Multiproduct SST trend (Figure 2b) was also observed in long-term trends computed from the NOAA OISST v2 product, with similar magnitudes (Lima & Wethey, 2012; Oliver et al., 2018). Such cooling has been attributed to multidecadal modes of variability related to a persistent La Niña state in the Pacific Ocean, which has been shown to have caused the recent hiatus in global average surface air temperatures during the first decade of the 21st century (England et al., 2014; Kosaka & Xie, 2013). The underlying warming trend in the eastern Pacific, visible in long-term SST reconstruction datasets (Lian et al., 2018), is therefore not captured within the recent 25 years. Despite this limitation, our results showed that internal variability was the main driver of MHW trends in the eastern Pacific (Figure 5) over the last 25 years. Although the long-term sign of change (negative) might be mis-represented in some regions by the limitations highlighted above, our findings highlight the large role that internal variability plays in driving MHW changes within several decades. In the case of the eastern Pacific, it is likely that the negative trends calculated from our record will become positive by including a few more years now that the climate hiatus has passed.

It is important to note that after removing the linear trends, an anthropogenic forcing signature likely remains in the SST internal variability signal. Climate change has not only been attributed to globally rising ocean temperatures, but it has also been identified as a major driver of frequency and intensity increase in some of the most important modes of climate variability such as ENSO (Wang et al., 2019) or the Pacific Decadal Oscillation (Jyoti et al., 2019) which in turn are likely to increase metrics of other marine extremes (Fasullo et al., 2018). Therefore, regions where MHW metric trends are better explained by internal variability changes are still likely to be influenced by climate change (in the projections to the end of this century) via modifications of internal variability processes locally.

Our study provides an overview of the representation of MHWs in different satellite SST products. To date, other MHW studies using daily satellite SST data have only considered the NOAA OISST product. Following a more robust ensemble approach, similar to the assessments from IPCC reports (Bindoff et al., 2014), we showed that there were no major differences between the datasets in the representation of the mean MHW state or MHW trends, except for MHW mean intensity. In contrast, there were important differences between products in identifying the main driver of MHW trends, indicating that MHW interannual variability differed among SST products. Note that here, we did not study the co-occurrence of events in different SST products, which could also prove important for the study of MHWs. These results suggest that although studying the mean state of MHWs does not require a specific choice of SST data set, scientists should be mindful of the characteristics of their satellite SST product of choice. Common satellite SST product biases arise from a multitude of factors including spatial and temporal resolution, instrumentation (microwave vs. infrared), calibration, and most importantly perhaps, differences in algorithm to define a specific depth of validity. Satellite observations typically measure the sea surface skin temperature which is highly impacted by subdaily variability due to heat exchanges between the ocean and the atmosphere. This layer is highly influenced by insolation and wind forcing rather than other dynamical forcing (Beggs, 2019). Some products use algorithms to reproduce the foundation temperature, to avoid subdaily contaminations. Algorithms differ among SST products but usually rely on suppressing subdaily variations of temperature by using observations at the local dawn time and/or using observations under well-mixed—moderate wind

conditions. For MGD, satellite data are rejected when the diurnal SST variation exceeds 3°. Differences in spatial resolution can also explain some discrepancies among products. Products with a resolution of 20 km can capture mesoscale variability but not entirely resolve it whereas finer resolution products, such as CCI (5 km), will likely resolve much finer scale processes, which can be of importance in coastal environments. Although results suggest that the mean and long-term trend state of MHWs are mildly impacted by product differences, spatial resolution differences can explain, in part, differences of SST internal variability. For those reasons, daily SST values can vary widely between products (Fiedler et al., 2019), and are only an estimation of the truth. This further highlights the virtues of the approach taken here. The use of multiple SST satellite products, each with different algorithms for analysis, cloud detection algorithms and gridding, reduces the systematic biases inherent to this type of observations.

There has been criticism around the use of SST in MHW studies, especially for assessing their impact on ecological systems. Subsurface temperature measurements might be more adequate to properly assess the impact of extreme heat events on ecosystems. Subsurface MHWs are likely to occur in most places with or without surface corresponding surface expressions (Elzahaby & Schaeffer, 2019; Schaeffer & Roughan, 2017). However, the ability to assess subsurface MHWs globally is limited by the sparsity and lack of continuity of such observations (Holbrook et al., 2020). Global ocean circulation models can be an alternative in providing continuous subsurface observations. Heat budget analysis derived from models are a valuable tool for tracing the sources of heat responsible for the development of MHWs (Holbrook et al., 2020). The role of vertical mixing, which is critical in redistributing heat from the surface to depths, and which satellite SST observations tend to overlook, can be quantified, along with ocean advection. While models have already been used to investigate the physical drivers of regional MHWs (Benthuysen et al., 2014; Chen et al., 2014; Kataoka et al., 2017; Li et al., 2020; Oliver et al., 2017), their utilization on a global scale could dramatically increase our understanding of MHWs driver and impact on ecological systems.

One of the aims of our study was not to provide an individual evaluation of SST products as it is evident that every product is different, but rather highlight that some biases in SST, and ultimately MHW characteristics, arise depending on the choice of product. Nevertheless, the major observed impacts of MHWs have been on marine ecosystems. The ocean skin layer thickness is typically a few millimeters, whereas foundation temperature is more representative of the temperature conditions that ecosystems are likely to be exposed to. Therefore, we suggest that satellite SST products defined at the foundation depth should be used in studies investigating ecological impacts of MHWs. For physical applications, scientists should be aware of the specificities of their satellite SST product of choice which can alter MHW metrics. When possible, an ensemble approach should be adopted as it minimizes the influence of product biases and enables a better estimation of the mean state.

5. Conclusion

The present MHW analysis forms a framework for coastal management and conservation policies in response to the increasing threat that MHWs impose on coastal marine ecosystems. Using an ensemble of long-term global SST reanalysis products, we identified the location of coastal MHW hotspots and estimated their associated change over the last 25 years. The highest MHW related threat was observed along the Mediterranean coastline, the north-eastern US coast and in some mid-latitudinal marginal seas like the Tasman and Japan Sea. Globally, increases in MHW exposure lead to increases in both short-term (individual events) and long-term MHW heat stress. Changes in the long-term mean SST were the main driver of the global observed increase of MHW metrics. This suggests that in the context of climate change, where marine ecosystems are clearly under threat (Bindoff et al., 2019), the MHW associated heat stress on coastal environments is likely to further increase dramatically, as global ocean temperatures are predicted to continue to warm during the 21st century and cross critical thresholds. The mean MHW state and its changes during the last 25 years were consistent across all satellite SST products used in this study, except for MHW mean intensity. Our study suggests, however, that there were critical differences in interannual variability of MHWs among products. This highlights the importance of the choice of satellite SST data in MHW applications, especially for individual event focus, and we recommend an ensemble approach to build the robustness of conclusions.

Data Availability Statement

The European Space Agency Climate Change Initiative and the Sea Surface Temperature Climate Change Initiative project together with the Centre for Environmental Data Analysis created and provided SST data available at https://catalogue.ceda.ac.uk/uuid/62c0f97b1eac4e0197a674870afe1ee6. CMC data were obtained from the National Aeronautics and Space Administration, Earth Observing System Data and Information System, Physical Oceanography Distributed Active Archive Center (PO.DAAC) at the Jet Propulsion Laboratory, Pasadena, CA (http://dx.doi.org/10.5067/GHGMR-4FJ01). The MGD data were obtained from the North-East Asian Regional Global Ocean Observing System (NEAR-GOOS) Regional Real Time Database (http://www.data.jma.go.jp/gmd/goos/data/pub/JMA-product/mgd_sst_glb_D/). OISST data were provided by the Physical Sciences Laboratory of National Oceanic and Atmospheric Administration/Earth System Research Laboratories, Boulder, Colorado (https://psl.noaa.gov/data/gridded/data.noaa.oisst.v2.highres.html).

Acknowledgments
The authors acknowledge agencies and organizations responsible for providing data. Maxime Marin and Ming Feng are partly supported by a CAS-CSIRO collaboration project on comparative studies of marine ecosystems between Australia and China.
Helen E. Phillips and Nathaniel L. Bindoff acknowledge funding from the Earth Systems and Climate Change Hub of the Australian Government's National Environmental Science Program.
Ming Feng is also supported by the Centre for Southern Hemisphere Oceans Research (CSHOR), which is a joint initiative between the Qingdao National Laboratory for Marine Science and Technology (QNLM), CSIRO, University of New South Wales and University of Tasmania.

References

Beggs, H. (2019). Chapter 12: Temperature. In B. A. Harrison, J. A. Anstee, A. Dekker, E. King, S. Phinn, N. Mueller, & G. Byrne (Eds.), *Earth observation: Data, processing and applications. Volume 3B: Applications—Surface waters*. Melbourne: CRCSI.

Benthuysen, J., Feng, M., & Zhong, L. (2014). Spatial patterns of warming off Western Australia during the 2011 Ningaloo Niño: Quantifying impacts of remote and local forcing. *Continental Shelf Research*, *91*, 232–246. https://doi.org/10.1016/j.csr.2014.09.014

Bindoff, N. L., Cheung, W. W. L., Kairo, J. G., Arístegui, J., Guinder, V. A., Hallberg, R., et al. (2019). Changing Ocean, Marine Ecosystems, and Dependent Communities. In H.-O. Pörtner, D. C. Roberts, V. Masson-Delmotte, P. Zhai, M. Tignor, E. Poloczanska, et al. (Eds.), *IPCC Special Report on the Ocean and Cryosphere in a Changing Climate* (pp. 450–545). In press.

Bindoff, N. L., Stott, P. A., AchutaRao, K. M., Allen, M. R., Gillett, N., Gutzler, D., et al. (2014). Detection and Attribution of Climate Change: from Global to Regional. *Climate Change 2013 – The Physical Science Basis: Working Group I Contribution to the Fifth Assessment Report of the Intergovernmental Panel on Climate Change*, (pp. 867–952). Cambridge University Press. https://doi.org/10.1017/CBO9781107415324.022

Bond, N. A., Cronin, M. F., Freeland, H., & Mantua, N. (2015). Causes and impacts of the 2014 warm anomaly in the NE Pacific. *Geophysical Research Letters*, *42*, 3414–3420. https://doi.org/10.1002/2015GL063306

Brasnett, B. (2008). The impact of satellite retrievals in a global sea-surface-temperature analysis. *Quarterly Journal of the Royal Meteorological Society*, *134*, 1745–1760. https://doi.org/10.1002/qj.319

Caputi, N., Kangas, M., Chandrapavan, A., Hart, A., Feng, M., Marin, M., & de Lestang, S. 2019. Factors affecting the recovery of invertebrate stocks from the 2011 Western Australian extreme marine heatwave. *Frontiers in Marine Science*, *6*, 484. https://doi.org/10.3389/fmars.2019.00484

Cavole, L., Demko, M. A., Diner, R., Giddings, A., Koester, I., Pagniello, C., et al. (2016). *Biological impacts of the 2013–2015 warm-water anomaly in the northeast Pacific: Winners, losers, and the future*. Washington, D.C: Oceanography.

Chen, K., Gawarkiewicz, G. G., Lentz, S. J., & Bane, J. M. (2014). Diagnosing the warming of the Northeastern U.S. Coastal Ocean in 2012: A linkage between the atmospheric jet stream variability and ocean response. *Journal of Geophysical Research: Oceans*, *119*, 218–227. https://doi.org/10.1002/2013JC009393

Collins, M., Sutherland, M., Bouwer, L., Cheong, S.-M., Fröliche, T., Combes, H. J. D., et al. (2019). Extremes, abrupt changes and managing risk. In H.-O. Pörtner, D. C. Roberts, V. Masson-Delmotte, P. Zhai, M. Tignor, E. Poloczanska, et al. (Eds.), *IPCC special report on the ocean and cryosphere in a changing climate*.

Costello, M. J., & Chaudhary, C. (2017). Marine biodiversity, biogeography, deep-sea gradients, and conservation. *Current Biology*, *27*, R511–R527. https://doi.org/10.1016/j.cub.2017.04.060

Elzahaby, Y., & Schaeffer, A. (2019). Observational insight into the subsurface anomalies of marine heatwaves. *Frontiers in Marine Science*, *6*, 745. https://doi.org/10.3389/fmars.2019.00745

England, M. H., McGregor, S., Spence, P., Meehl, G. A., Timmermann, A., Cai, W., et al (2014). Recent intensification of wind-driven circulation in the Pacific and the ongoing warming hiatus. *Nature Climate Change*, *4*, 222–227. https://doi.org/10.1038/nclimate2106

Fasullo, J. T., Otto-Bliesner, B. L., & Stevenson, S. (2018). ENSO's changing influence on temperature, precipitation, and wildfire in a warming climate. *Geophysical Research Letters*, *45*, 9216–9225. https://doi.org/10.1029/2018GL079022

Feng, M., Hendon, H. H., Xie, S.-P., Marshall, A. G., Schiller, A., Kosaka, Y., et al. (2015). Decadal increase in Ningaloo *Niño* since the late 1990s. *Geophysical Research Letters*, *42*, 104–112. https://doi.org/10.1002/2014GL062509

Feng, M., McPhaden, M. J., Xie, S.-P., & Hafner, J. (2013). La Niña forces unprecedented Leeuwin Current warming in 2011. *Scientific Reports*, *3*, 1277. https://doi.org/10.1038/srep01277

Fiedler, E. K., McLaren, A., Banzon, V., Brasnett, B., Ishizaki, S., Kennedy, J., et al. (2019). Intercomparison of long-term sea surface temperature analyses using the GHRSST Multi-Product Ensemble (GMPE) system. *Remote Sensing of Environment*, *222*, 18–33. https://doi.org/10.1016/j.rse.2018.12.015

Garrabou, J., Coma, R., Bensoussan, N., Bally, M., Chevaldonne, P., Cigliano, M., et al. (2009). Mass mortality in Northwestern Mediterranean rocky benthic communities: Effects of the 2003 heat wave. *Global Change Biology*, *15*, 1090–1103. https://doi.org/10.1111/j.1365-2486.2008.01823.x

Gilmour, J. P., Smith, L. D., Heyward, A. J., Baird, A. H., & Pratchett, M. S. (2013). Recovery of an isolated coral reef system following severe disturbance. *Science*, *340*(80), 69–71. https://doi.org/10.1126/science.1232310

Hobday, A. J., Alexander, L. V., Perkins, S. E., Smale, D. A., Straub, S. C., Oliver, E. C. J., et al. (2016). A hierarchical approach to defining marine heatwaves. *Progress in Oceanography*, *141*, 227–238. https://doi.org/10.1016/j.pocean.2015.12.014

Holbrook, N. J., Scannell, H. A., Sen Gupta, A., Benthuysen, J. A., Feng, M., Oliver, E. C. J., et al. (2019). A global assessment of marine heatwaves and their drivers. *Natural Communications*, *10*, 1–13. https://doi.org/10.1038/s41467-019-10206-z

Holbrook, N. J., Sen Gupta, A., Oliver, E. C. J., Hobday, A. J., Benthuysen, J. A., Scannell, H. A., et al. (2020). Keeping pace with marine heatwaves. *Nature Reviews Earth & Environment*, *1*, 482–493. https://doi.org/10.1038/s43017-020-0068-4

Hughes, T. P., Kerry, J. T., Álvarez-Noriega, M., Álvarez-Romero, J. G., Anderson, K. D., Baird, A. H., et al. (2017). Global warming and recurrent mass bleaching of corals. *Nature*, *543*, 373–377. https://doi.org/10.1038/nature21707

Jacox, M. G. (2019). Marine heatwaves in a changing climate. *Nature*, *571*, 485–487. https://doi.org/10.1038/d41586-019-02196-1

Jyoti, J., Swapna, P., Krishnan, R., & Naidu, C. V. (2019). Pacific modulation of accelerated south Indian Ocean sea level rise during the early 21st Century. *Climate Dynamics*, *53*, 4413–4432. https://doi.org/10.1007/s00382-019-04795-0

Kataoka, T., Tozuka, T., & Yamagata, T. (2017). Generation and decay mechanisms of Ningaloo Niño/Niña. *Journal of Geophysical Research: Oceans*, *122*, 8913–8932. https://doi.org/10.1002/2017JC012966

Kosaka, Y., & Xie, S.-P. (2013). Recent global-warming hiatus tied to equatorial Pacific surface cooling. *Nature*, *501*, 403–407. https://doi.org/10.1038/nature12534

LaJeunesse, T. C., Parkinson, J. E., Gabrielson, P. W., Jeong, H. J., Reimer, J. D., Voolstra, C. R., & Santos, S. R. (2018). Systematic revision of Symbiodiniaceae highlights the antiquity and diversity of coral endosymbionts. *Current Biology*, *28*, 2570–2580. https://doi.org/10.1016/j.cub.2018.07.008

Lian, T., Shen, Z., Ying, J., Tang, Y., Li, J., & Ling, Z. (2018). Investigating the uncertainty in global SST trends due to internal variations using an improved trend estimator. *Journal of Geophysical Research: Oceans*, *123*, 1877–1895. https://doi.org/10.1002/2017JC013410

Li, Z., Holbrook, N. J., Zhang, X., Oliver, E. C. J., & Cougnon, E. A. (2020). Remote forcing of Tasman Sea marine heatwaves. *Journal of Climate*, *33*, 5337–5354.

Lima, F. P., & Wethey, D. S. (2012). Three decades of high-resolution coastal sea surface temperatures reveal more than warming. *Nature Communications*, *3*, 704. https://doi.org/10.1038/ncomms1713

Liu, G., Strong, A. E., & Skirving, W. (2003). Remote sensing of sea surface temperatures during 2002 Barrier Reef coral bleaching. *Eos Transactions, American Geophysical Union*, *84*, 137–141. https://doi.org/10.1029/2003EO150001

Lough, J. M., Anderson, K. D., & Hughes, T. P. (2018). Increasing thermal stress for tropical coral reefs: 1871–2017. *Scientific Reports*, *8*, 6079. https://doi.org/10.1038/s41598-018-24530-9

Merchant, C. J., Embury, O., Bulgin, C. E., Block, T., Corlett, G. K., Fiedler, E., et al. (2019). Satellite-based time-series of sea-surface temperature since 1981 for climate applications. *Scientific Data*, *6*, 223. https://doi.org/10.1038/s41597-019-0236-x

Oliver, E. C. J. (2019). Mean warming not variability drives marine heatwave trends. *Climate Dynamics*, *53*, 1653–1659. https://doi.org/10.1007/s00382-019-04707-2

Oliver, E. C. J., Benthuysen, J. A., Bindoff, N. L., Hobday, A. J., Holbrook, N. J., Mundy, C. N., & Perkins-Kirkpatrick, S. E. (2017). The unprecedented 2015/16 Tasman Sea marine heatwave. *Nature Communications*, *8*, 16101. https://doi.org/10.1038/ncomms16101

Oliver, E., Burrows, M., Donat, M., Gupta, A., Alexander, L., Perkins-Kirkpatrick, S., et al. (2019). Projected marine heatwaves in the 21st Century and the potential for ecological impact. *Frontiers in Marine Science*, *6*, 734. https://doi.org/10.3389/fmars.2019.00734

Oliver, E. C. J., Donat, M. G., Burrows, M. T., Moore, P. J., Smale, D. A., Alexander, L. V., et al. (2018). Longer and more frequent marine heatwaves over the past century. *Nature Communications*, *9*, 1324. https://doi.org/10.1038/s41467-018-03732-9

Pearce, A., Lenanton, R., Jackson, G., Moore, J., Feng, M., & Gaughan, D. (2011). The "marine heat wave" off Western Australia during the summer of 2010/11. In *Fisheries Research Report* (Vol. 222, p. 40). Western Australia: Department of Fisheries.

Reynolds, R. W., Smith, T. M., Liu, C., Chelton, D. B., Casey, K. S., & Schlax, M. G. (2007). Daily high-resolution-blended analyses for sea surface temperature. *Journal of Climate*, *20*, 5473–5496. https://doi.org/10.1175/2007JCLI1824.1

Sakurai, T., Yukio, K., & Kuragano, T. (2005). Merged satellite and in-situ data global daily SST. In *Proceedings. 2005 IEEE International Geoscience and Remote Sensing Symposium, 2005. IGARSS '05* (pp. 2606–2608).

Santoso, A., Mcphaden, M. J., & Cai, W. (2017). The defining characteristics of ENSO extremes and the strong 2015/2016 El Niño. *Reviews of Geophysics*, *55*, 1079–1129. https://doi.org/10.1002/2017RG000560

Scannell, H., Pershing, A., A.M, A., Thomas, A. C., & Mills, K. E. (2016). Frequency of marine heatwaves in the North Atlantic and North Pacific since 1950. *Geophysical Research Letters*, *43*(5), 2069–2076.

Schaeffer, A., & Roughan, M. (2017). Subsurface intensification of marine heatwaves off southeastern Australia: The role of stratification and local winds. *Geophysical Research Letters*, *44*, 5025–5033. https://doi.org/10.1002/2017GL073714

Smale, D. A., & Wernberg, T. (2013). Extreme climatic event drives range contraction of a habitat-forming species. *Proceedings of the Royal Society B: Biological Sciences*, *280*, 20122829. https://doi.org/10.1098/rspb.2012.2829

Sparnocchia, S., Schiano, M. E., Picco, P., Bozzano, R., & Cappelletti, A. (2006). The anomalous warming of summer 2003 in the surface layer of the Central Ligurian Sea (Western Mediterranean). *Annales Geophysicae*, *24*, 443–452. https://doi.org/10.5194/angeo-24-443-2006

Thomas, L., López, E. H., Morikawa, M. K., & Palumbi, S. R. (2019). Transcriptomic resilience, symbiont shuffling, and vulnerability to recurrent bleaching in reef-building corals. *Molecular Ecology*, *28*, 3371–3382. https://doi.org/10.1111/mec.15143

Vecchi, G. A., & Harrison, D. E. (2006). The termination of the 1997–98 El Niño. Part I: Mechanisms of oceanic change. *Journal of Climate*, *19*, 2633–2646. https://doi.org/10.1175/JCLI3776.1

Wang, B., Luo, X., Yang, Y.-M., Sun, W., Cane, M. A., Cai, W., et al. (2019). Historical change of El Niño properties sheds light on future changes of extreme El Niño. *Proceedings of the National Academy of Sciences*, *116*(45), 22512–22517. https://doi.org/10.1073/pnas.1911130116

Wernberg, T., Smale, D. A., Tuya, F., Thomsen, M. S., Langlois, T. J., de Bettignies, T., et al. (2012). An extreme climatic event alters marine ecosystem structure in a global biodiversity hotspot. *Nature Climate Change*, *3*, 78. https://doi.org/10.1038/nclimate1627

Wessel, P., & Smith, W. H. F. (1996). A global, self-consistent, hierarchical, high-resolution shoreline database. *Journal of Geophysical Research*, *101*, 8741–8743.

Zhang, N., Feng, M., Hendon, H. H., Hobday, A. J., & Zinke, J. (2017). Opposite polarities of ENSO drive distinct patterns of coral bleaching potentials in the southeast Indian Ocean. *Scientific Reports*, *7*, 2443. https://doi.org/10.1038/s41598-017-02688-y

Zhao, Z., & Marin, M. (2019). A MATLAB toolbox to detect and analyze marine heatwaves software. *Journal of Open Source Software*. *4*(33), 1124. https://doi.org/10.21105/joss.01124